Bioorganic & Medicinal Chemistry 22 (2014) 4371–4375

Contents lists available at ScienceDirect

Bioorganic & Medicinal Chemistry

journal homepage: www.elsevier.com/locate/bmc

A C-14 labeled Py–Im polyamide localizes to a subcutaneous prostate cancer tumor

Jevgenij A. Raskatov, James W. Puckett, Peter B. Dervan *

Division of Chemistry and Chemical Engineering, California Institute of Technology, Pasadena, CA 91125, United States

ARTICLE INFO

Article history:
Received 14 February 2014
Accepted 6 April 2014
Available online 16 April 2014

Keywords:
C-14 radiolabeling
Small molecule
DNA binding
Accumulation
Chemotherapy

ABSTRACT

In an effort to quantitate Py–Im polyamide concentrations in vivo, we synthesized the C-14 radioactively labeled compounds **1**–**3**, and investigated their tumor localization in a subcutaneous xenograft model of prostate cancer (LNCaP). Tumor concentrations were compared with representative host tissues, and exhibited a certain degree of preferential localization to the xenograft. Compound accumulation upon repeated administration was measured. Py–Im polyamide **1** was found to accumulate in LNCaP tumors at concentrations similar to the IC_{50} value for this compound in cell culture experiments.

1. Introduction

Py–Im polyamides are a modular class of organic molecules, which can be programmed to recognize defined DNA sequences with affinities and specificities comparable to those of DNA binding proteins.[1] Focused molecular tuning identified positive determinants of cellular uptake for Py–Im polyamides.[2] Ensuing gene regulation studies demonstrated the potential of these molecules to occlude binding of various transcription factors, such as the androgen receptor,[3] the hypoxia inducible factor,[4] and the nuclear factor kappa-B.[5] Importantly, the mode of action of Py–Im polyamides is not limited to the transcription factor DNA interface. Recent in vitro studies established that Py–Im polyamides can induce inhibition of the RNA polymerase II activity with subsequent degradation of the protein, as well as p53 stress response induction, without accompanying DNA damage.[6] We were able to demonstrate that Py–Im polyamides are bioavailable following an intravenous,[7] intraperitoneal or a subcutaneous injection,[8] and are taken up by tumors in vivo.[9] Subsequent investigations established their antitumor effects in an LNCaP tumor xenograft model.[6,10] This provided an incentive to develop an approach to quantitate compound levels in tumor xenografts, and to compare those with representative tissues of the animal host in vivo.[11]

Radioactive C-14 labeling allows to synthesize traceable organic molecules without altering their chemical properties. The approach enables the observation of in vivo compound uptake for a relatively prolonged period of time with a wider range of concentrations, as opposed to the more commonly used LC/MS/MS quantitation methods. Consequentially, this technique was put to advantage in investigating biodistribution and metabolism of diverse molecular classes, comprising small molecules,[12] proteins,[13] and antibody–drug conjugates.[14] The present account reports the synthesis and biodistribution of three C-14 labeled Py–Im polyamides in an in vivo tumor xenograft model.

2. Results

2.1. Py–Im polyamide 1 exhibits preferential xenograft localization

The radioactive, C-14 labeled, eight-ring hairpin Py–Im polyamide **1** (ImPyPyPy-(R)$^{\alpha\text{-NHAc}}$γ-ImPyPyPy) that codes for the DNA sequence 5′-WGWWCW-3′ was of particular interest for the investigation (Fig. 1). This stems from its recently demonstrated antitumor activity in a subcutaneous prostate cancer xenograft model (LNCaP), which was accompanied by reduced animal toxicity, as compared to closely related molecules.[10] An initial set of single dose experiments was conducted, with tissue harvest performed 24 h past compound administration. In order to compare the tumor-associated levels of Py–Im polyamide **1** with its distribution to the animal, host kidney, liver and lung were chosen as representative organs. A mean tumor-associated concentration of **1** was measured as 1.48 mg/kg, which corresponds to 1.06 μM (Fig. 2A). Substantially lower concentrations were observed for kidney and lung (0.25 and 0.12 mg/kg, respectively). The liver displayed a concentration of 1.04 mg/kg of compound **1**, which is 29% lower than that established in tumors ($p < 0.01$).

* Corresponding author. Tel.: +1 626 395 6002; fax: +1 626 683 8753.
E-mail address: dervan@caltech.edu (P.B. Dervan).

http://dx.doi.org/10.1016/j.bmc.2014.04.010
0968-0896/

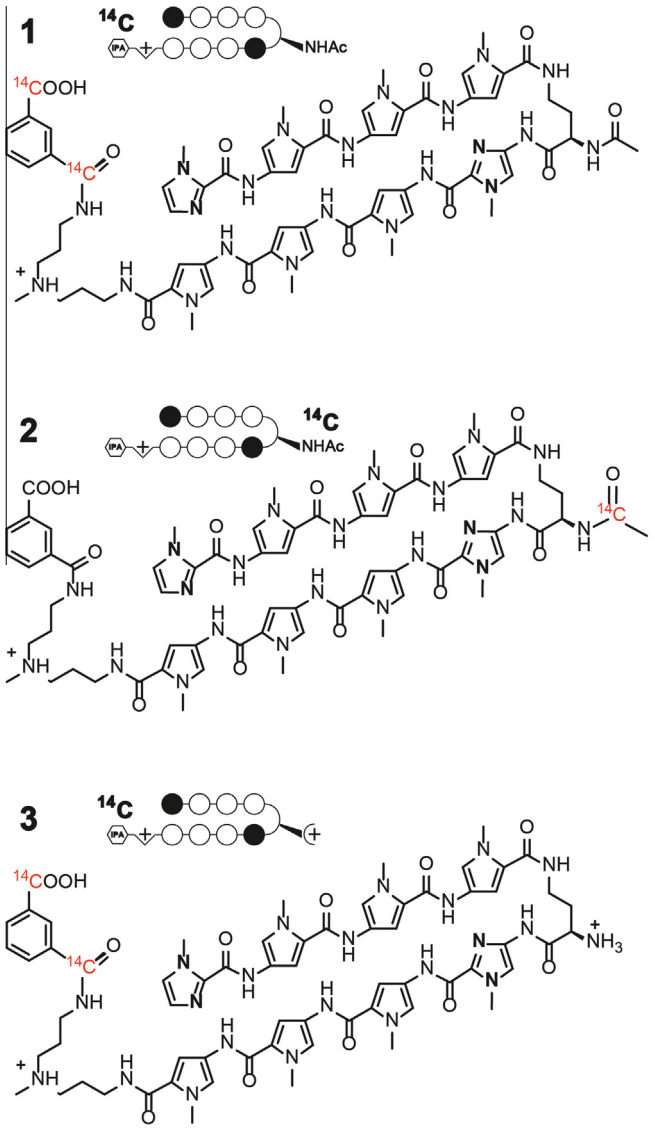

Figure 1. Chemical structures and ball-and-stick representations of the C-14 radioactively labeled hairpin Py–Im polyamides **1**–**3** employed in the study.

2.2. Differentially labeled Py–Im polyamide 2 suggests limited degradation in vivo

To probe for potential metabolic loss of the C-14 radiolabeled isophthalic acid (IPA) terminus of Py–Im polyamide **1** in vivo, the differentially radiolabeled compound **2** was synthesized. The molecule **2** is chemically identical to **1**, but carries the C-14 radioactive label at the acetate of the α-acetamide-GABA linker unit instead of the IPA moiety (Fig. 1), thus allowing to probe for compound decomposition. In both the tumor tissue, as well as for the representative host tissues chosen, the corresponding mean values were determined to be within experimental error between the compounds **1** and **2** (Fig. 2B and Supporting information, Fig. SI1, top panel).

2.3. In vivo biodistribution of Py–Im polyamide 1 is superior to analogue 3

Antitumor activity against LNCaP in a subcutaneous xenograft mouse model was initially demonstrated with the non-radioactive version of the Py–Im polyamide **3**.[6] Subsequent studies established an improved therapeutic index of its acetylated analogue **1**.[10] The synthesis and administration of radioactively labeled compound **3** (Fig. 1) for comparison to the biodistribution values measured for Py–Im polyamide **1** was therefore of high interest (Fig. 2A and C). Whereas tumor-associated levels were within error between the two molecules, substantially higher levels of **3** were noted for all host tissues examined (Supporting information, Fig. SI1, bottom panel). Particularly striking was the difference in lung levels, which was almost eightfold higher with **3** (0.12 and 0.93 mg/kg for compounds **1** and **3**, respectively).

2.4. In vivo biodistribution of Py–Im polyamide 1 as a function of post-injection time

In order to gain insight into the uptake and clearance rates of **1** from tumor and the reference host organs chosen, four different post-injection time points were examined (Fig. 3). The 4 h time point was chosen to represent the scenario in which compound **1** is still in circulation.[10] In addition to the 24 h time point, more prolonged exposure time frames were investigated (3 and 7 days, respectively). At the earliest time point probed, Py–Im polyamide **1** exhibited some twofold enrichment in the tumor over all host tissues probed. There was no notable difference between the levels measured for the host kidney, liver and lung, thus pointing towards a comparable degree of their vascularization and penetration by **1**. Interestingly, a markedly different profile was observed 24 h post-exposure. Liver values were found to be substantially higher than those of kidney (4.2-fold) or lung (8.7-fold). Kidney and lung tissues were found to clear Py–Im polyamide **1** at substantially higher rates than the liver, not much of a change being noted for the latter between 4 and 24 h (Fig. 3). At prolonged exposure times of up to 7 days, tissue levels of **1** were found to diminish consistently, dropping to 0.45 mg/kg (tumor), 0.05 mg/kg (kidney), 0.27 mg/kg (liver)

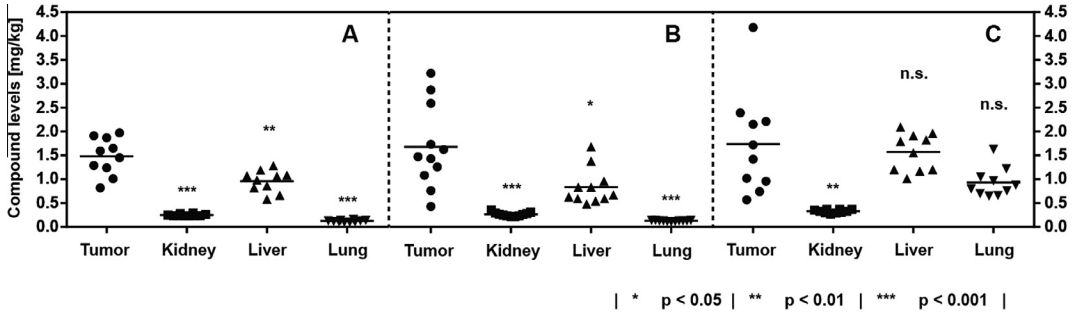

Figure 2. Compound levels of the C-14 radioactively labeled Py–Im polyamides **1** (A), **2** (B) and **3** (C) in subcutaneously grafted LNCaP tumors, compared with representative major animal host tissues (kidney, liver and lung). Each datapoint represents an individual organ analyzed. All injections were performed intraperitoneally at 20 nmol per animal (NSG male mouse; *N* = 10 in each group) and tissues harvested 24 h following administration. Quantitation was conducted by liquid scintillation counting. Statistical comparison was conducted against tumor levels of compounds **1**–**3**.

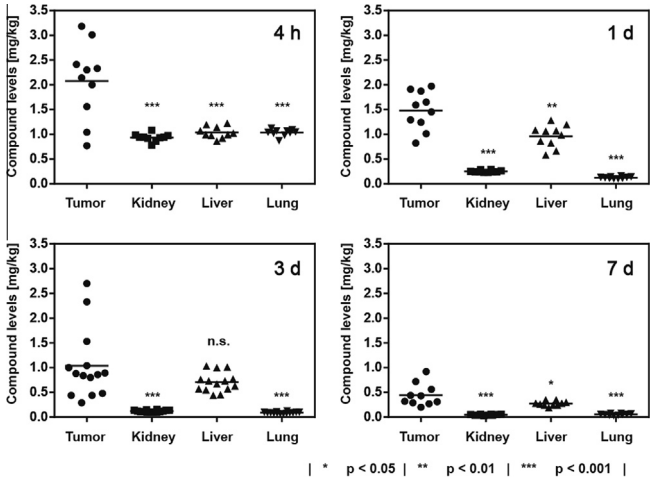

Figure 3. Compound levels of C-14 labeled Py–Im polyamide **1** in LNCaP tumor and representative organs at varying post-injection time points. All injections were performed intraperitoneally at 20 nmol per animal (NSG male mouse; $N \geqslant 10$). Quantitation was conducted by liquid scintillation counting of the organ harvested at the indicated time point. Statistical comparison was conducted against tumor levels of compound **1**.

and 0.06 mg/kg (lung). The radioactively labeled Py–Im polyamide **1** was still readily detectable in all tissues 7 days after its injection (Figs. 3 and 4).

2.5. Multiple injections of Py–Im polyamide 1 lead to compound accumulation

Given that our published treatment schedules consist of at least three injections with compound typically administered every 2–3 days,[9,10] probing for compound accumulation under such conditions was clearly of interest.

A multiple exposure experiment was conducted, following the treatment schedule displayed in Figure 5. Tissue levels of compound **1** were found to be consistently higher than those observed in single injection experiments. Comparison with the 24 h time point revealed that **1** accumulated at concentrations ranging from 1.8-fold (liver and kidney) to 2.4-fold (tumor) higher following three injections. Single injection experiments with longer exposure time points displayed consistently lower compound levels.

3. Discussion

The C-14 radiolabeling approach represents a sensitive way of creating readily detectable molecules with an extended tracer lifetime, without altering their chemical properties. The technology has been highly valuable in investigating medicinally important small molecules of relevance to the treatment of cancer and other diseases. Examples encompass the toxin colchicine,[15] the antidiabetic candidate muraglitazar,[16] the DNA-binding cytotoxic agent doxorubicin,[17] the camptothecin analogue lurtotecan,[18] and the mitotic inhibitor paclitaxel.[19] The quantitative approach using radiolabeled polyamides allows determining, at least in part, their pharmacokinetic and pharmacodynamic parameters. A preceding study from our laboratory employed ^{18}F labeling, which allows tracing molecules in vivo, employing the non-invasive positron emission tomography imaging technology.[11] An 8-ring hairpin polyamide coding for the sequence 5′-WTWCGW-3′ was evaluated, revealing liver accumulation and GI-effected compound excretion as some key findings. However, ^{18}F being a short-lived radionuclide ($t_{1/2}$ of 109.8 min), the ^{18}F-labeled compound was only traced for 2 h following injection. In order to shed light onto chemotherapeutic potential of polyamides, substantially more extended time points are required. This is afforded by employing the ^{14}C labeling technique, which is the focus of the present study. The findings can be correlated with the tumor growth attenuation, as well as animal toxicity.[10] Furthermore, insight can be gained into their mechanistic mode of action in vivo. Both aspects are of high significance for translational research, as discussed below.

A. Chemotherapeutic aspects: An ideal chemotherapeutic in cancer therapy should exert its cytotoxic activity at the tumor site exclusively, without causing damage to any healthy host tissues. This hypothetical scenario is not achieved with any of the currently

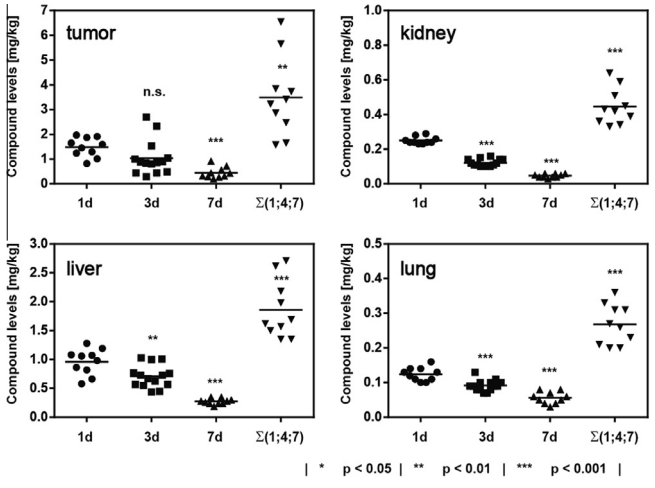

Figure 4. Compound levels of C-14 labeled Py–Im polyamide **1** in LNCaP tumor and representative organs, presented in a time-resolved fashion. Compound levels are compared against their respective levels measured at the 1 day timepoint for all organs. Repeated injections (rightmost columns) display substantial accumulation. All injections were performed intraperitoneally at 20 nmol per animal (NSG male mouse). Quantitation was conducted by liquid scintillation counting. Each datapoint represents an individual organ analyzed. Statistical comparison was conducted against tumor levels of compound **1**. Σ(1;4;7) denotes the accumulation experiment; see also Figure 5.

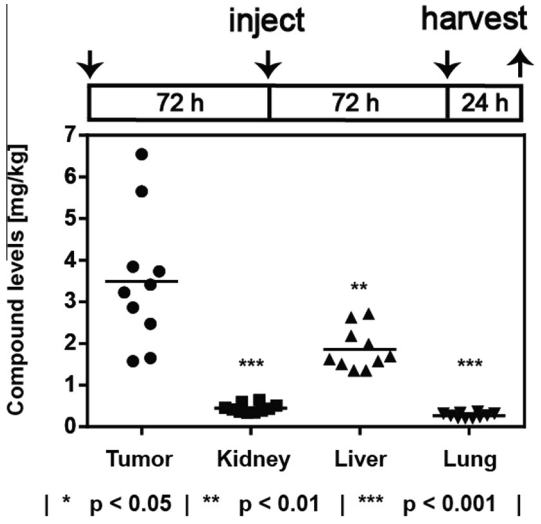

Figure 5. Compound levels of C-14 labeled Py–Im polyamide **1** in LNCaP tumor and representative organs following three injections on days 1, 4 and 7 of the experiment. Compound was administered intraperitoneally at 20 nmol per animal per injection (NSG male mouse). Harvest was performed 24 h following the last injection. Quantitation was conducted by liquid scintillation counting. Each datapoint represents an individual organ analyzed. Statistical comparison was conducted against tumor levels of compound **1**.

approved drugs. Remarkable advances have been reported for the treatment of neoplasias that possess well-characterized genomic lesions, which are indispensable for tumor proliferation. Notable improvements in treatment of advanced prostate cancer have been achieved over the past decade. Novel FDA-approved therapeutics encompass the aromatase inhibitor abiraterone,[20] the inhibitor of androgen receptor (AR) signaling enzalutamide,[21] and radium-223, which is an alpha-emitting radiopharmaceutical applied in the treatment of prostate cancer-derived bone metastases.[22] A key step towards the emergence of high-grade, castration-resistant prostate cancer involves point mutations in androgen receptor. One such mutation (W741C) results in the reversal of the antagonistic effect the antiandrogen drug bicalutamide, whereas other mutations can lead to the activation of mutant AR in a ligand-independent manner.[23] Enzalutamide behaves as an antagonist of both the wild-type and, in contrast to bicalutamide, the W741C mutant androgen receptor and prevents its translocation into the nucleus, thereby disrupting an assembly of the functional transcription factor complex. Despite the remarkable progress in targeting advanced prostate cancer, however, a large portion of the chemotherapeutic repertoire remains to be represented by relatively non-specific cytotoxins.[24] Py–Im polyamide **1** targets the consensus ARE and should also prevent binding of both wild-type and W741C mutant androgen receptors to DNA. Such an approach could, in principle, be immune to further mutations in AR.

The comparison of Py–Im polyamide tissue concentrations to those of other C-14 labeled DNA binding drugs enable the contextualization of the pK profile of **1**. Quantitative in vivo data from C-14 labeling experiments exist for the clinically approved chemotherapeutic doxorubicin, which warrants an explicit comparison to the present investigation. A subcutaneous xenograft model was conducted for the MCF7 cell line, with doxorubicin injected intraperitoneally at 1.6 mg/kg.[17] This is close to the quantities of the C-14 labeled Py–Im polyamides administered in the present study (20 nmol of **1** injected into an animal with a typical weight of 30 g corresponds to a 0.93 mg/kg dose). The authors of the doxorubicin study reported tumor localization values of about 1 mg/kg for their xenografts, monitored for up to 24 h after a single injection. We measured values of about 1.5 mg/kg for the compounds **1**–**3** at the 24 h timepoint. This can be considered encouraging, given that doxorubicin is a clinically approved chemotherapeutic.

A drastic difference is noted for the liver-associated compound values. Whereas the liver levels of compound **1** did not change markedly between the 4 and 24 h time point, and were considerably lower than the tumor levels at both time points (2-fold and 1.5-fold, respectively), doxorubicin was found to localize to the liver at levels some 2-fold higher than those measured for the MCF7 xenografts initially (2 h timepoint), but then to clear rapidly. Given the chemical reactivity of doxorubicin, metabolic processing appears likely, and may in fact give rise to toxic intermediates that are devoid of the C-14 label. In our study, Py–Im polyamide **1** was found to clear slowly (over the course of 7 days) and at comparable rates from both the LNCaP xenografts and the host organs assessed, thus suggesting non-specific clearance rather than metabolic processing. This interpretation is further supported by the data obtained with the differentially labeled compound **2**, which yielded values comparable to those of **1** at the 24 h timepoint, thus underscoring the stability of this Py–Im polyamide in vivo.

Some twofold accumulation of **1** was observed upon repeated injection in both the tumor and the animal organs assessed. Whereas the tumor accumulation is an asset of the molecule, the organ retention prompts a note of caution. Advanced delivery strategies, such as nanoparticle formulations or tumor-homing moieties, could be employed to reduce host organ accumulation.[25] Amelioration of doxorubicin toxicity in a liposomal (cardiolipin) formulation has been previously demonstrated to result in an altered organ distribution, with consistently lower tissue compound levels measured for the cardiolipin formulation.[26]

Comparison of Py–Im polyamide **1** with the closely related analog **3** reveals that the acetylated compound **1** exhibits some 2-fold reduced host tissue levels without affecting the concentration in the LNCaP xenografts, which is clearly an advance for translation aspects. This allows to rationalize an aspect of the preceding study, namely that a single injection of the non-radioactive version of **3**, but not **1**, at 10 mg/kg resulted in liver toxicity.[10] Overall, the study demonstrates the value of subtle molecular variation in improving molecular in vivo properties of drug candidates.

B. Mechanistic aspects: We measured a mean tumor concentration of 3.49 mg/kg (2.50 μM) in the multiple injection experiment (Fig. 5), which is remarkably close to the IC_{50} value measured for the non-radioactive version of **1** in LNCaP cell culture (2.1 μM).[10] This is not inconsistent with direct cytotoxic action of the compound upon the tumor, as opposed to an indirect effect, which could stem from disrupting the nutrient supply due to systemic host toxicity, or from the interference with host growth hormone production (e.g., testosterone). The question that remains is whether the compound exerts its cytotoxic effects directly on the xenografted LNCaP cells or does so by disrupting the tumor microenvironment. These two scenarios would lead to the same functional readout, namely attenuation of tumor proliferation. They therefore cannot be readily distinguished with the C-14 labeling method, because averaged whole-tumor compound levels are obtained.

It should be kept in mind that, although the in vivo tumor-levels measured for **1** are close to the IC_{50} measured in cell culture for the non-radioactive version of the compound, an explicit comparison between a cell culture study and an in vivo experiment is a problematic one. In a xenograft experiment, a complex and dynamic interface is formed between the grafted (human) cell line and the host animal. The interface encompasses angiogenesis, infiltration by various immune cells (even the heavily immunosuppressed NSG mice still possess some functional aspects of the innate immunity wing) and hormone signaling, inter alia. It is further complicated by the fact that in cell culture, the compound exposure is invariant over the experimental time frame, while an oscillatory profile is expected in tumors due to clearance. Correspondingly, the concentration of 2.5 μM, which was measured in the accumulation experiment 24 h after administration of Py–Im polyamide, is likely to somewhat underestimate the peak tumor levels that are reached. Finally, xenografts are heterogenous in nature, and as such spatial variance of compound levels within an individual tumor can be expected. Genetically engineered tumor models (e.g., the TRAMP mouse) tend to recapitulate the host-tumor interface more accurately than xenograft models, and may hence be of value in shedding light onto mechanism of action of Py–Im polyamides in future in vivo studies.[27]

4. Conclusion

Three C-14 radioactively labeled Py–Im polyamides were synthesized and their levels quantitated in subcutaneous LNCaP xenografts following intraperitoneal administration. The measured compound levels were compared with representative host samples (kidney, liver and lung). An up to 12-fold preferential tumor localization (compared to lung) was measured for the Py–Im polyamide **1** and its differentially labeled chemical equivalent **2**, but not for the charged analog **3**. This demonstrates the value of small molecule modifications to improve therapeutic index of drug candidates, and is in line with preceding toxicity studies.[10] Upon repeated administration (three injections over 7 days), compound **1** exhibited some twofold accumulation in all tissues examined. Comparison with **2** suggested that metabolic processing does not

play a significant role over the time period probed. The tumor levels of **1** that were achieved in the accumulation experiment are comparable to the IC_{50} measured for the LNCaP cell line in culture.

4.1. Materials and methods

4.1.1. Synthesis of radioactively labeled compounds

The core for the Py–Im polyamides **1–3** was synthesized on resin, following previously reported procedures.[28] Radioactive building blocks were obtained from ARC and conjugated to Py–Im polyamide intermediates following standard protocols (Supporting information, Fig. SI2). All compounds were quantitated by liquid scintillation counting prior to injection, employing the activity constants of 55 mCi/mmol (isophthalic acid) and 25 mCi/mmol (acetate), as provided by the vendor of radioactive materials. All spectra were quench-corrected using a standard curve that was produced employing Beckman C-14 standards and defined quantities of nitromethane as the quenching agent (Supporting information, Fig. SI3). All compounds were confirmed single peaks (purity >99%) by analytical HPLC and co-eluted with the corresponding non-radiolabeled materials as additional quality control.

4.1.2. Cell culture and in vivo experimentation

The LNCaP cell line was obtained from ATCC and cultured following the vendor's recommendations. Cells were not allowed to exceed passage number 25. Engraftment was only performed, where cell viability exceeded 90% by trypan blue staining. Male NSG mice were obtained from JAX and housed in a level A animal facility in accordance with IACUC regulations. Cells were grafted subcutaneously (flank) in 200 μL of a 1:1 mixture cell culture media and matrigel at 2.5 M per inoculation. Tumor growth was monitored weekly. Animals were administered the radioactively labeled compound 4–8 weeks after engraftment in a specifically dedicated fume hood that was set up for C-14 radioexperimentation. Where exposure exceeded 24 h, animals were transferred to an isolated facility with regulated temperature, humidity and a light-dark cycle, and removed for terminal procedures as needed. In order to ensure optimal hydration of animals, gelpacks were supplied once in three days in addition to the standard water bottles. All animals were housed in disposable cages, which were destroyed at the end of the experiment, following established radiosafety protocols. Animals were euthanized by CO_2 asphyxiation at gas pressures of 2–3 atm. Tumors of varying sizes were evaluated, the majority falling between 25 and 200 mg upon excision, although occasional outliers in both directions were present. No correlation was noted between tumor size and compound accumulation (Supporting information, Fig. SI4).

4.1.3. Tissue solubilization and quantitation of Py–Im polyamide levels

Tumors, kidneys, livers and lungs were excised, rinsed with PBS and the residual washing liquid absorbed on paper towels. Single samples typically did not exceed 300 mg per solubilization experiment. Individual samples were placed into scintillation vials and 1 mL SOLVABLE (Perkin Elmer) added. Vials were subsequently placed into an incubator (+55 °C) for a minimal incubation period of 12 h. Samples were removed from the incubator, allowed to cool to ambient temperature and 2 × 200 μL of an aqueous hydrogen peroxide solution added (30% w/w, Sigma–Aldrich). Once there was no further visible evolution of gas, the samples were placed back into the incubator for an additional hour. They were subsequently allowed to cool back down to ambient temperature and 10 mL of the scintillation fluid HIONIC-FLUOR (Perkin Elmer) added per vial. Scintillation counting was performed on a Beckman Coulter LS6500 Multi-Purpose Scintillation Counter. All values were quench-corrected using IC# in conjunction with the quench curve (Supporting information, Fig. SI3) and normalized for initial organ weight.

Acknowledgments

JAR is grateful to the Alexander von Humboldt foundation for the award of a Feodor Lynen postdoctoral fellowship. Professor Bogdan Olenyuk is gratefully acknowledged for helpful discussion. We are indebted to Dr. Janet Baer, Dr. Karen Lencioni and Dr. Haick Issaian for their help with technical aspects of experimental design. We are grateful for support by the National Institutes of Health (GM51747 and GM27681).

Supplementary data

Supplementary data (additional statistical analyses, synthetic schemes, scatter plots of tumor compound levels as a function of tumor weight, and a liquid scintillation counting quench curve) associated with this article can be found, in the online version, at http://dx.doi.org/10.1016/j.bmc.2014.04.010.

References and notes

1. (a) Dervan, P. B.; Edelson, B. S. *Curr. Opin. Struct. Biol.* **2003**, *13*, 284; (b) Kielkopf, C. L.; White, S.; Szewczyk, J. W.; Turner, J. M.; Baird, E. E.; Dervan, P. B.; Rees, D. C. *Science* **1998**, *282*, 111; (c) White, S.; Szewczyk, J. W.; Turner, J. M.; Baird, E. E.; Dervan, P. B. *Nature* **1998**, *391*, 468.
2. (a) Edelson, B. S.; Best, T. P.; Olenyuk, B.; Nickols, N. G.; Doss, R. M.; Foister, S.; Heckel, A.; Dervan, P. B. *Nucl. Acids Res.* **2004**, *32*, 2802; (b) Nickols, N. G.; Jacobs, C. S.; Farkas, M. E.; Dervan, P. B. *Nucl. Acids Res.* **2007**, *35*, 363.
3. Nickols, N. G.; Dervan, P. B. *Proc. Natl. Acad. Sci. U.S.A.* **2007**, *104*, 10418.
4. Nickols, N. G.; Jacobs, C. S.; Farkas, M. E.; Dervan, P. B. *ACS Chem. Biol.* **2007**, *2*, 561.
5. Raskatov, J. A.; Meier, J. L.; Puckett, J. W.; Yang, F. T.; Ramakrishnan, P.; Dervan, P. B. *Proc. Natl. Acad. Sci. U.S.A.* **2012**, *109*, 1023.
6. Yang, F.; Nickols, N. G.; Li, B. C.; Marinov, G. K.; Said, J. W.; Dervan, P. B. *Proc. Natl. Acad. Sci. U.S.A.* **2013**, *110*, 1863.
7. Synold, T. W.; Xi, B. X.; Wu, J.; Yen, Y.; Li, B. C.; Yang, F.; Phillips, J. W.; Nickols, N. G.; Dervan, P. B. *Cancer Chemother. Pharmacol.* **2012**, *70*, 617.
8. Raskatov, J. A.; Hargrove, A. E.; So, A. Y.; Dervan, P. B. *J. Am. Chem. Soc.* **2012**, *134*, 7995.
9. Raskatov, J. A.; Nickols, N. G.; Hargrove, A. E.; Marinov, G. K.; Wold, B.; Dervan, P. B. *Proc. Natl. Acad. Sci. U.S.A.* **2012**, *109*, 16041.
10. Yang, F.; Nickols, N. G.; Li, B. C.; Szablowski, J. O.; Hamilton, S. R.; Meier, J. L.; Wang, C.-M.; Dervan, P. B. *J. Med. Chem.* **2013**, *56*, 7449.
11. Harki, D. A.; Satyamurthy, N.; Stout, D. B.; Phelps, M. E.; Dervan, P. B. *Proc. Natl. Acad. Sci. U.S.A.* **2008**, *105*, 13039.
12. McCarthy, K. E. *Curr. Pharm. Des.* **2000**, *6*, 1057.
13. Davis, L. D. R.; Spencer, W. J.; Pham, V. T.; Ward, T. L.; Blais, D. R.; Mack, D. R.; Kaplan, H.; Altosaar, I. *Anal. Biochem.* **2011**, *410*, 57.
14. Kitson, S. L.; Quinn, D. J.; Moody, T. S.; Speed, D.; Watters, W.; Rozzell, D. *Chim. Oggi* **2013**, *31*, 29.
15. Mehta, B. M.; Rosa, E.; Biedler, J. L.; Larson, S. M. *J. Nucl. Med.* **1994**, *35*, 1179.
16. Li, W. Y.; Zhang, D. L.; Wang, L. F.; Zhang, H.; Cheng, P. T.; Zhang, D. X.; Everett, D. W.; Humphreys, W. G. *Drug Metab. Dispos.* **2006**, *34*, 807.
17. Raghunand, N.; Mahoney, B. P.; Gillies, R. *Biochem. Pharmacol.* **2003**, *66*, 1219.
18. Emerson, D. L. et al *Clin. Cancer Res.* **2000**, *6*, 2903.
19. Varma, M. V. S.; Panchagnula, R. *Eur. J. Pharm. Sci.* **2005**, *25*, 445.
20. De Bono, J. S. et al *N. Eng. J. Med.* **2011**, *364*, 1995.
21. Scher, H. I. et al *N. Eng. J. Med.* **2012**, *367*, 1187.
22. Parker, C. et al *N. Eng. J. Med.* **2013**, *369*, 213.
23. Hara, T.; Miyazaki, J.; Araki, H.; Yamaoka, M.; Kanzaki, N.; Kusaka, M.; Miyamoto, M. *Cancer Res.* **2003**, *63*, 149.
24. Cavalli, F. *Textbook of Medical Oncology*, 4th ed.; Informa: Boca Raton, 2009.
25. Ruoslahti, E.; Bhatia, S. N.; Sailor, M. J. *J. Cell Biol.* **2010**, *188*, 759.
26. Rahman, A.; Carmichael, D.; Harris, M.; Roh, J. K. *Cancer Res.* **1986**, *46*, 2295.
27. (a) Frese, K. K.; Tuveson, D. A. *Nat. Rev. Cancer* **2007**, *7*, 645; (b) Martiniello-Wilks, R.; Dane, A.; Mortensen, E.; Jeyakumar, G.; Wang, X. Y.; Russell, P. *J. Anticancer Res.* **2003**, *23*, 2633; (c) Sharma, P.; Schreiber-Agus, N. *Oncogene* **1999**, *18*, 5349.
28. Puckett, J. W.; Green, J. T.; Dervan, P. B. *Org. Lett.* **2012**, *14*, 2774.